Flow asymmetry in geometrically symmetric engine head configurations

M. Węcław, A. Melling and F. Durst
Lehrstuhl für Strömungsmechanik (LSTM), Universität Erlangen-Nürnberg, Erlangen, F.R. Germany

Flow visualization using oil-streak techniques and velocity measurements by laser-Doppler anemometry were used to provide detailed information on the inlet flow in the cylinder of a research (model) engine head under steady flow conditions. The inlet port and valve geometry were arranged in such a way that a plane of symmetry existed for the geometry. Nevertheless, asymmetric flow resulted inside the cylinder. The measurements demonstrated that a valve location off the cylinder axis always results in asymmetric flow patterns inside the cylinder. The flow asymmetry increases with increased valve offset and increased valve lift.

Keywords: internal flows; flow asymmetry; flow visualization; LDA; reciprocating engines

1. Introduction

The flow structure and its development in the cylinder during the intake stroke is strongly influenced by the geometry of the engine head, the inlet valve, and the inlet port. Information exists on the effects of geometrical parameters on the inlet flow (Monaghan and Pettifer 1981; Hirotomi et al. 1981; Brandstätter, Johns, and Wigley 1985; Lee et al. 1992); however, the phenomenon of asymmetric flow in symmetric geometries has not been investigated. Further, detailed fluid-flow information is needed to improve the engine performance (Arcoumanis and Whitelaw 1987), as well as to understand the nature of the intake process. Also, from the point of view of computational fluid dynamics (CFD), it is, e.g., necessary to know whether the in-cylinder flow is symmetrically distributed around the geometrical symmetry plane.

As the simplest case, the flow field for an axisymmetric cylinder geometry has been investigated in the literature by means of flow visualization, laser-Doppler anemometry, and numerical calculations under both steady and motored test conditions (Gosman et al. 1978; Ahmadi-Befrui, Gosman, and Watkins 1984; Gosman, Johanbakhsh, and Watkins 1985; Takenaka et al. 1990), as well as in a water analog engine (Ekchian and Hoult 1979). Experimental work has also been done for nonaxisymmetric head configurations with off-axis valve location using a water analog engine (Ekchian and Hoult 1979; Kent et al. 1989; Khalighi 1990) and with air flow (Arcoumanis et al. 1984). Computations (Paul 1987) have shown that for an off-axis valve, nonaxisymmetric contact of the induction jet with the cylinder wall makes in-cylinder flow very complex, and difficult to compute. A more recent attempt (Tsui and Lee 1992) to compute the flow at the valve gap, using steady flow conditions and an idealized axisymmetric port-valve configuration, showed that details of the flow such as the size of the separation zone could not be predicted accurately.

An inlet port investigated by Lee et al. (1992) is generally similar to the one used in the present paper. Considering, however, a difference in the port offset from the cylinder axis and a different shape of the port (short converging inlet), a rather different flow pattern is produced in the cylinder. Some similar flow features were nevertheless found in the near cylinder wall and head face areas.

In a recent paper, Węcław, Melling, and Durst (1993) have shown that surface flow mapping techniques permit an insight into the flow close to the cylinder head and the cylinder walls, as well as over the valve head and in the intake port. The main advantage of the technique is a quick comparison of time-average flow patterns for different head geometries and valve and intake pipe configurations. Extending this information by detailed velocity-profile measurements in selected parts of the cylinder provides insight into the entire flow field. Going from the idealized case of an axisymmetric engine head configuration (on-axis inlet port) to a more realistic engine geometry (geometrically symmetric head configuration with a bent inlet port and an off-axis valve), this paper presents an extended investigation of the degree of the in-cylinder flow asymmetry.

The test rig, engine head configurations, and experimental methods for flow visualization and flow velocity measurements are described in section 2. Results by the surface mapping techniques and by laser-Doppler anemometry are presented in section 3. Results are given in section 3.1 for an on-axis valve. The asymmetric flow field for an off-axis valve in a symmetric geometry is discussed in section 3.2. Flow asymmetry for an intake port without valve is described in section 3.3. In section 3.4, the flow asymmetry for several geometrically symmetric engine head configurations are presented for three valve lifts, yielding increasingly asymmetric flows in the cylinder as the valve lift increases. Conclusions are drawn in section 4.

Address reprint requests to Dr. Węcław at Lehrstuhl für Strömungsmechanik (LSTM), Universität Erlangen-Nürnberg, Caverstr. 4, D-91058 Erlangen, F.R. Germany.

Received 12 August 1993; accepted 9 February 1994

2. Head configurations and instrumentation

2.1. Head configurations

For the investigations, an idealized engine head was designed to allow easy change of valve location in the cylinder, valve lift, and intake port azimuthal orientation. Three geometrically symmetric head configurations have been investigated: on-axis valve ($S = 0$), half of maximum valve offset ($S = 0.5$ max) and "maximum" offset (S = max) (see Figure 1). Additionally, the case of maximum offset without intake valve has been investigated. A research engine head was used with a directed intake port of constant circular cross-sectional area. Head parameters like intake port azimuthal orientation, valve offset, or valve diameter can be investigated. Because the inlet valve geometry significantly influences the initial conditions for the in-cylinder flow development, in the present investigations two inlet valve geometries were used: a production valve (type I) characterized by a sharp edge between the valve head and sealing faces, and a valve of the same diameter but simpler geometry without any edge (type II) (see Figure 1). An intake pipe of diameter $D_p = 0.8D$ was used, where D is the valve diameter. The intake pipe had a straight length of $3D_p$ followed by a 90° bend of radius $1.5D_p$ before entering the cylinder.

2.2. Steady-flow test rig

The steady-flow test rig includes a research engine head and transparent Plexiglas cylinder of diameter 90 mm, allowing optical access. A blower sucks air through the engine head and the cylinder. The mass flow rate is measured by a turbine flowmeter and is regulated by a set of valves. The overall pressure drop through the intake port is measured as an average value from four taps around the cylinder in the plane 230 mm from the engine head.

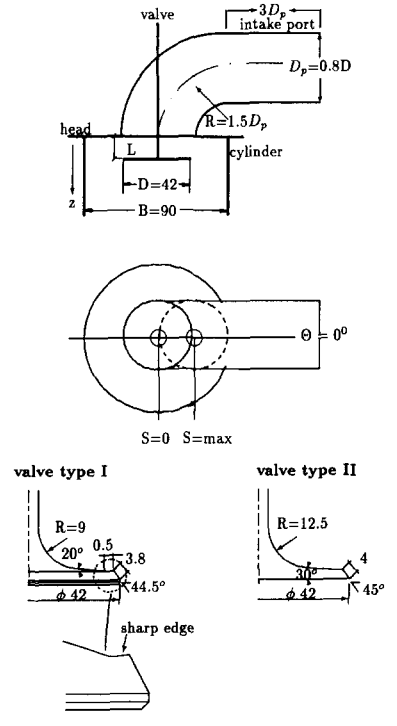

Figure 1 Engine head configurations and two geometries of the inlet valve

The results reported in this paper were obtained under constant-pressure-drop conditions $\Delta p = 1960$ Pa and $\Delta p = 2490$ Pa, corresponding to bulk velocities in the cylinder (for maximum valve lift) $V_b = 5.7$ m/s and 6.5 m/s, respectively. These velocities correspond to engine speeds (for typical bore-to-stroke ratios) on the order of 3200 rpm and 3700 rpm, respectively.

2.3. LDA system

For velocity measurements, a fiber optic laser-Doppler anemometer (Stieglmeier and Tropea 1992) was used with a miniaturized fiber probe. An argon-ion laser with an output power of 400 mW provided sufficient power for backscatter measurements. The laser beam was split using a Bragg cell, which also introduced a frequency shift between the two beams to facilitate measurements in highly turbulent flow. The laser light was transmitted to the probe using monomode fibers, which maintain the TEM_{00} mode of the laser resonator and the polarization of the coherent laser light. A multimode fiber was used to transmit scattered light collected from the LDA measurement volume back to an avalanche photodiode, allowing a high transmission for noncoherent scattered light and easy coupling of the fibers. A short focal length ($f = 60$ mm) of the probe lens was used to maximize the signal-to-noise ratio in the near cylinder wall velocity measurements. Main specifications of this configuration are the following: beam crossing angle: 15.19°; measuring volume length: 136 μm; measuring volume diameter: 18 μm; and fringe spacing: 1.95 μm. The velocity component was selected by rotating the probe of the one-component anemometer.

The intake flow was seeded around the intake pipe inlet by a mixture of nebulizer fluid and water from a six-jet atomizer. As signal processor, a counter (TSI 1990) was used. An ensemble-average technique for the LDA data processing was used. The velocity gradient broadening was minimized by using very small measuring volume dimensions. The estimated uncertainty for velocity was $\delta U \leq 0.15$ m/s and the uncertainty for the radial position of the measuring volume in the cylinder was 100 μm.

2.4. Oil-streak technique

For the time-averaged wall flow patterns, an oil-streak flow-visualization technique was used in order to "freeze" the flow pattern on the cylinder head, the valve head, and the cylinder wall. This method uses an oil-pigment mixture that has to run to completion until the oil has either evaporated or stopped moving. It is assumed that the pigment streaks left behind closely follow the air surface streamlines. Steady separation lines are seen as mixture accumulations, and attachment lines may be seen as areas free of pigment and the source of stream lines (Węcłaś, Melling, and Durst 1993).

The working mixture consisted of toner, transparent high-viscosity oil, and petroleum. Volume ratios of these components had to be chosen to suit the flow conditions. For flow visualization, the cylinder head and the valve were painted with the working mixture and the flow pattern was "frozen" during 180 seconds of flow. For the cylinder wall, a thin, stiff, transparent foil cylinder was pressed into the Plexiglas cylinder and then painted with the working mixture. The foil cylinder was held in the Plexiglas cylinder with a very thin high-viscosity oil film to prevent relative displacement of the cylinders during flow. The mixture was also injected into the intake pipe (instead of painting the walls) to get a time-averaged flow pattern representing the discharge from the valve and emphasizing the positive flow away from the cylinder head.

3. Flow asymmetry for different geometrically symmetric head configurations

3.1. Near-axisymmetric flow for on-axis valve

Results already reported by Węcłaś, Melling, and Durst (1993) (for the same intake port as used in this paper) showed that for an on-axis valve, the flow is close to axisymmetric, even when the intake port contains a 90° bend. The axial velocity in the cylinder was characterized by the formation of an almost symmetrically distributed recirculation zone over about two thirds of the cylinder cross section. Near-zero net swirl flow was also found, with significant tangential velocities only close to the cylinder wall along the diameter perpendicular to the port orientation. Close to the head, secondary flows at the cylinder wall-head corner introduced some asymmetry. As flow visualization showed, however, the valve jet impinged symmetrically on the cylinder wall around the cylinder axis, in spite of flow separation around the valve stem and a preference for the flow to follow the outer radius of the intake pipe bend.

For an axisymmetric head geometry, Ekchian and Hoult (1979) and Khalighi (1990) in a water analog engine have confirmed axisymmetric flow and the existence of the vortex in the top corner of the cylinder. Flow modeling by Gosman (1985) has also shown negative mean axial velocity over a wide region of the flow.

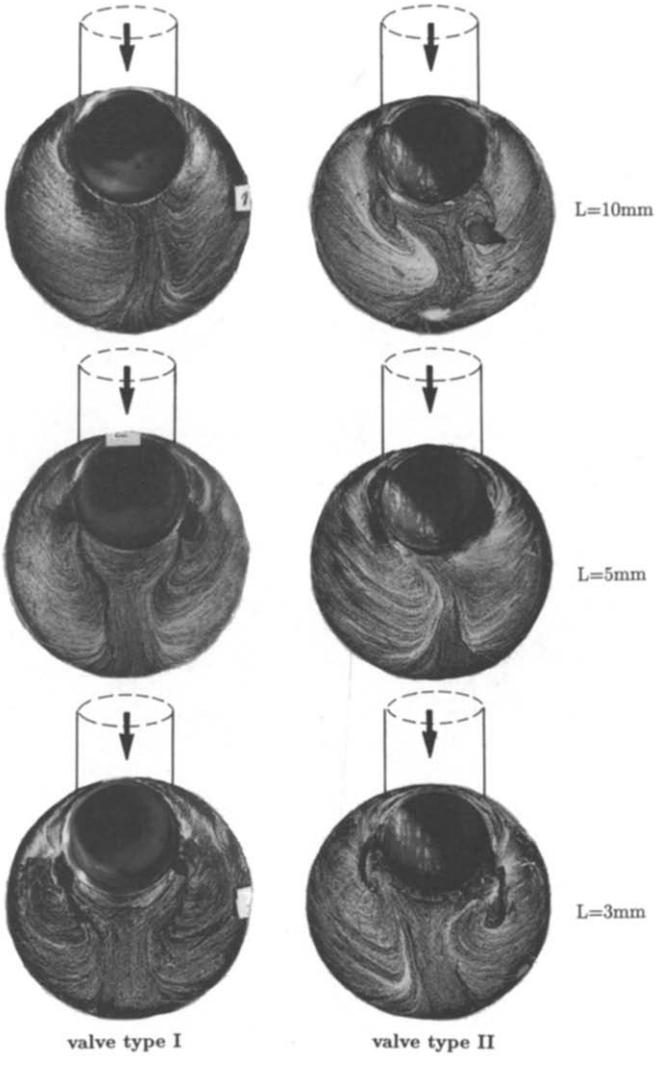

Figure 2 Time-averaged flow pattern on the cylinder head face for maximum valve offset and three lifts, for two valve geometries ($\Delta p = 2490$ Pa)

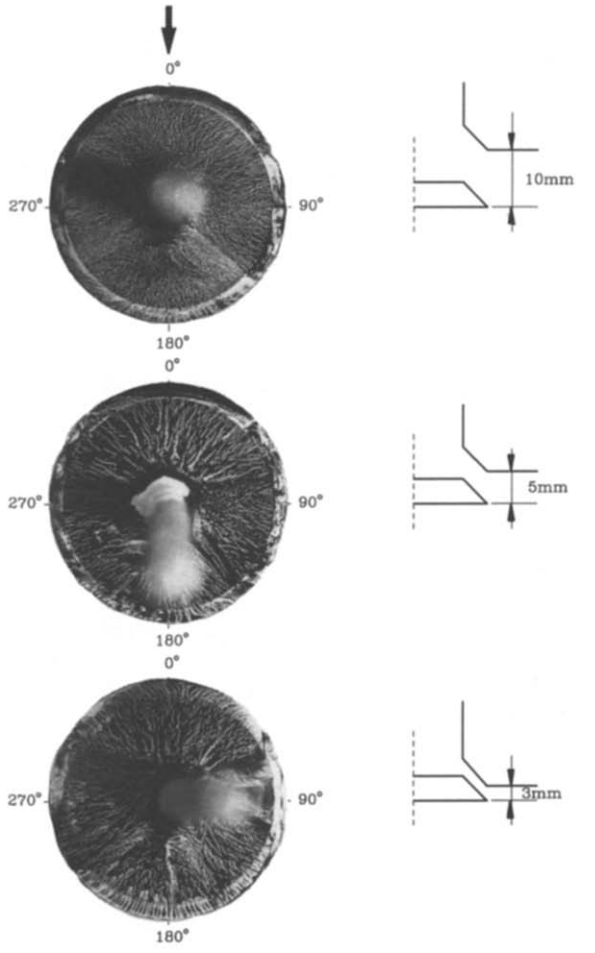

Figure 3 Time-averaged flow pattern on the valve head for maximum valve offset and three valve lifts (valve type II, $\Delta p = 2490$ Pa). Arrow indicates port direction

3.2. Asymmetric flow for off-axis valve

3.2.1. Surface flow visualization. For geometrically symmetric head configurations with off-axis valve location, the flow in the cylinder is not symmetric. The degree of asymmetry is influenced by the valve lift and axial distance from the head. A qualitative indication of the flow asymmetry may be obtained rapidly using surface flow visualization. For maximum offset (Figure 2), the time-averaged flow patterns on the cylinder head for three valve lifts and the two valve geometries of Figure 1 are visualized for 2490 Pa pressure drop. The symmetry improves with valve lift reduction. Slight differences in the valve geometry lead to different flow separations in the valve gap, which influence the in-cylinder flow structure. The present surface flow visualization suggests that the mechanism of these separations is too complex to be represented by a simple four-modes model (Tsui and Lee 1992; Tanaka 1929; Annand and Roe 1974) of flow separation in the valve gap.

Flow separation at the valve sealing face may be observed in time-averaged flow patterns on the valve head (type II) for three lifts in Figure 3. The dark regions on the valve sealing face represent flow separation, and bright streak lines represent attached flow. The inlet port is orientated along the 0°–180°

line. With this valve geometry, the smooth border between the valve head and sealing faces minimizes the flow separations at the valve. At maximum valve lift (Figure 3a), flow separates from the valve sealing face around 0° at the inner port radius location with most of the air flowing over the surface of the valve opposite the port orientation. On the opposite side of the valve head, flow separation lines are indicated with nonradial streak lines between them, corresponding to the main flow region in the intake port. This figure also shows a highly nonuniform discharge around the symmetry line.

At half of the maximum lift (Figure 3b), the azimuthal range of flow separation on the sealing face around the 0° point is significantly reduced, and the discharge around the valve periphery becomes more symmetric than at maximum valve lift. Around 180°, i.e., oppositely orientated from the intake port, the streak lines are continuous between valve head and sealing face. This feature is even clearer at low lift (L = 3 mm; see Figure 3c), where no separations at the sealing face are observed, and the streak lines are continuous except around 90° and 270°. At these angles, i.e., in the plane perpendicular to the inlet port axis, there is probably impingement between the flows along the internal and external port radii. The continuity of the streak lines between the valve head and sealing face indicates flow attachment to the valve at low lifts, due to dominant viscous effects at low Reynolds numbers. At low valve lifts, as suggested in the literature (Arcoumanis and Whitelaw 1987; Tsui and Lee 1992; Tanaka 1929; Kahlighi, El Tahry, and Kuziak 1986), the flow also attaches to the valve seat face. This was confirmed by streak-line analysis on the cylinder head face around the seat area.

The present investigations indicate that flow separation in the valve gap must be analyzed as a function not only of the valve lift but also of the inlet port azimuthal orientation and valve location with respect to the cylinder wall. The flow asymmetry did not result from any inaccuracy of the inlet-port azimuthal orientation with respect to the geometrical symmetry plane. The tangential velocity near 180° and close to the cylinder wall was not zero, and could not be reduced to zero (as expected for symmetric flow) by small changes in the

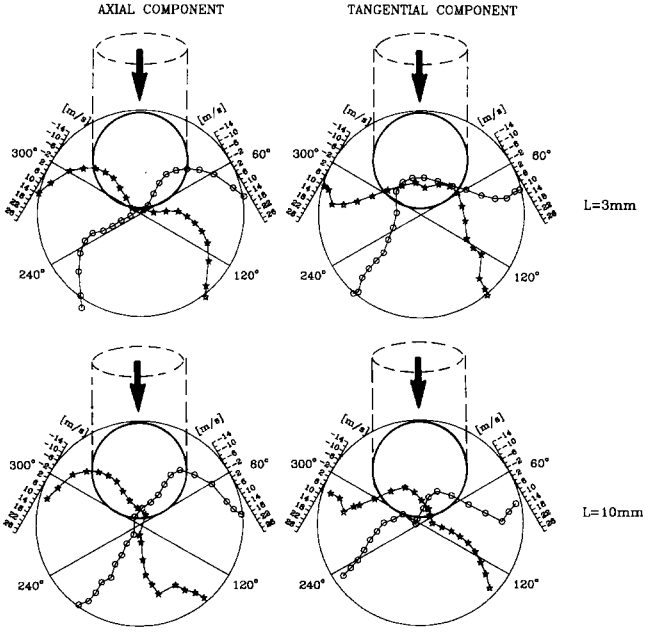

Figure 4 Axial and tangential velocity distributions along the two symmetrical cross sections for two valve lifts (valve type I, Δp = 2490 Pa)

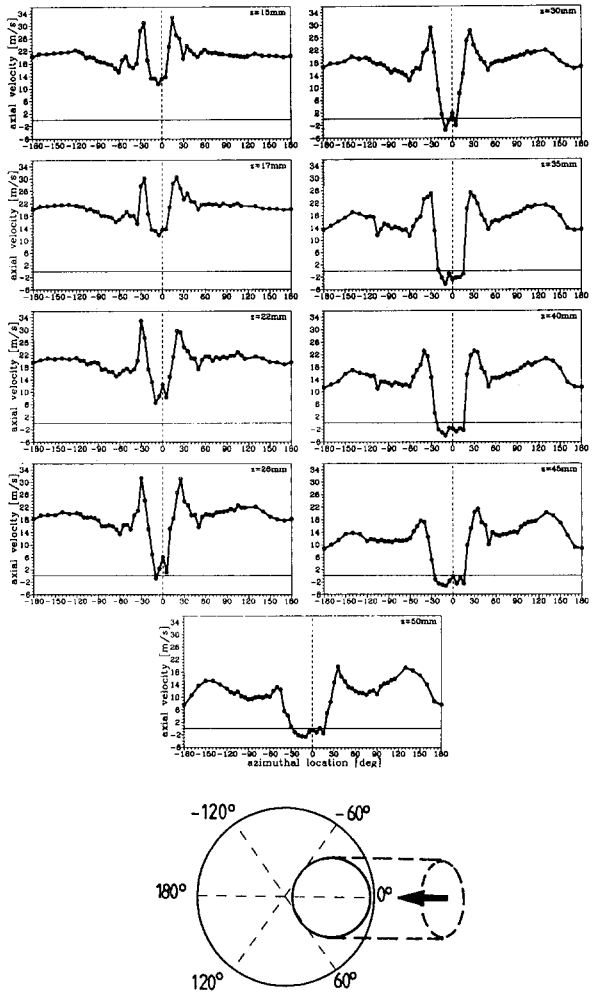

Figure 5 Axial velocity distribution around the cylinder periphery at different axial distances from the head (0°-symmetry line) measured 1 mm from the cylinder wall for maximum valve offset and valve lift L = 3 mm (valve type I, Δp = 1960 Pa)

intake-port azimuthal angle around the symmetry plane. Finally, it is noted that for the type I valve, continuous streak lines were found only at extremely low lifts (about 1 mm), indicating the effect of the more pronounced boundary between the valve head and sealing faces with this valve.

3.2.2. Velocity measurements. Point measurements by LDA allow the degree of asymmetry to be quantified, but data in a large number of cross sections are required. For two symmetrically distributed sections around the geometrical symmetry plane, the axial and tangential velocity components at the distance half of the cylinder bore from the head are shown for low and maximum valve lifts (valve type I) in Figure 4, and clearly demonstrate the flow asymmetry.

Surface flow visualization on the cylinder wall for off-axis valve location indicated asymmetric contact of the valve jets with the cylinder wall. To quantify this asymmetry, the axial velocity was measured around the cylinder periphery at 1 mm in radial distance from the cylinder wall. The measurements were taken for the type I valve at maximum valve offset and low valve lift (L = 3 mm). In the range of 0° to ±120°, the azimuthal spacing between points was 5°, and at higher angles 10°. The axial velocity distributions along the cylinder periphery at different axial distances from the head are shown in Figure 5. These distributions may be described in the

following ranges of azimuthal location:

1°. Small angles around 0°, where the distributions are characterized by the lowest velocities, asymmetrically distributed around the symmetry plane. At higher distances from the head, the width of this range increases, and reverse velocities are encountered.
2°. Slightly higher azimuthal locations, where the velocity increases rapidly; the velocity peaks on both sides of the symmetry plane are similar, but their azimuthal locations are asymmetric.
3°. Angles (approx. $\pm 60°$), where the velocity drops to a local minimum.
4°. High azimuthal angles (toward $\pm 180°$), where the velocity distribution is very flat at low distances from the head, but slightly convex around $\pm 120°$ to $\pm 150°$ at high distance from the head.

At all axial distances, the most rapid azimuthal variations in velocity are observed at low angles, i.e., in the part of the cylinder near the valve. At higher distances from the head, the zone of significant azimuthal velocity variations is extended toward 180°. As reported elsewhere (Węcłaś, Melling, and Durst 1993), along the 0°-line down the cylinder, the flow changes from a strong positive wall jet at low distances from the head, through an area of unsteady local flow characterized by periodic alternation between two states of flow, to a recirculating flow far from the engine head. The transition between the two flow states contributes to an apparently high turbulence intensity level of the axial flow with maxima located at small angles on both sides of the symmetry plane. The azimuthal distribution of the turbulence intensity near the cylinder wall was almost independent of the axial distance. The area of flow characterized by periodic flow unsteadiness is related to the flow separation area. From this point of view, surface flow visualization is still useful, clearly indicating where separation exists in the flow. However, detailed quantitative analysis of flow requires LDA measurements, as was done by Węcłaś, Melling, and Durst (1993).

3.3. Flow generated by the inlet port without valve

In the light of the above results, it was important to investigate whether the flow asymmetry could come from a small eccentricity of valve location in the inlet port. Thus the flow generated by the inlet port with removed valve was examined for signs of asymmetry. Axial velocity profiles measured across two sections in the cylinder, symmetrically distributed around the inlet port axis, at 21 mm from the cylinder head under 1960 Pa test conditions are shown in Figure 6. The flow is not symmetrically distributed around the symmetry plane; however, in the central part of the cylinder, the asymmetry is

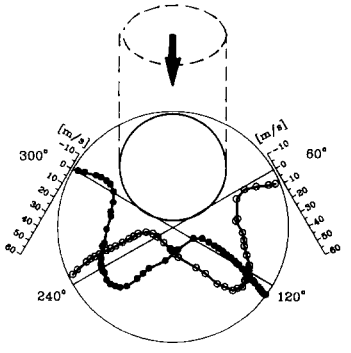

Figure 6 Axial velocity distribution across the cylinder at $z = 21$ mm from the cylinder head for the intake port with removed valve at maximum offset and $\Delta p = 1960$ Pa

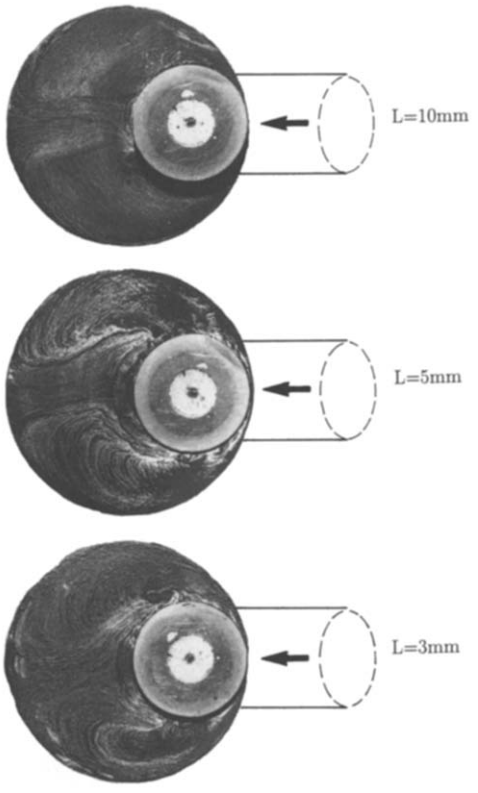

Figure 7 Time-averaged flow pattern on the cylinder head face for three valve lifts and maximum valve offset (valve type 1, $\Delta p = 1960$ Pa)

very small. The main differences occur in the outer part of the cylinder, especially on the opposite side from the port location in the head.

The time-averaged flow pattern on the cylinder head was recorded and showed a slightly asymmetric flow in the outer part of the cylinder. Analysis of the streak lines at the valve seat face showed asymmetric discharge from the port into the cylinder (probably due to the bend of the inlet port) as well as a discontinuity of the streaks between the cylinder head face and the seat, indicating flow separation at the outflow from the port. Additionally, a significant back-flow into the port in the region around the inner port radius was observed.

The results suggest that for off-axis port location, an asymmetric flow in the cylinder, as observed in the flow pattern on the cylinder wall, is not a result of a small eccentricity of the valve. Rather, the asymmetry seems to develop in the bend of the intake port, and could also be influenced by flow blockage by the cylinder wall for high valve offsets.

3.4. Flow asymmetry for three valve offsets and three lifts

Flow separations in the valve gap influence the valve surface flow distribution (section 3.2), the discharge coefficient (Arcoumanis and Whitelaw 1987; Tanaka 1929; Annand and Roe 1974)—which is strongly influenced by the pressure drop, especially at lower valve lifts—and the flow asymmetry in the cylinder. In this section, oil-streak flow visualization results are compared for valve type I at three valve offsets and three lifts with configurations as in section 3.2 but with a lower pressure drop $\Delta p = 1960$ Pa.

In the case of maximum valve offset, the time-averaged flow patterns on the cylinder head face are shown in Figure 7. At

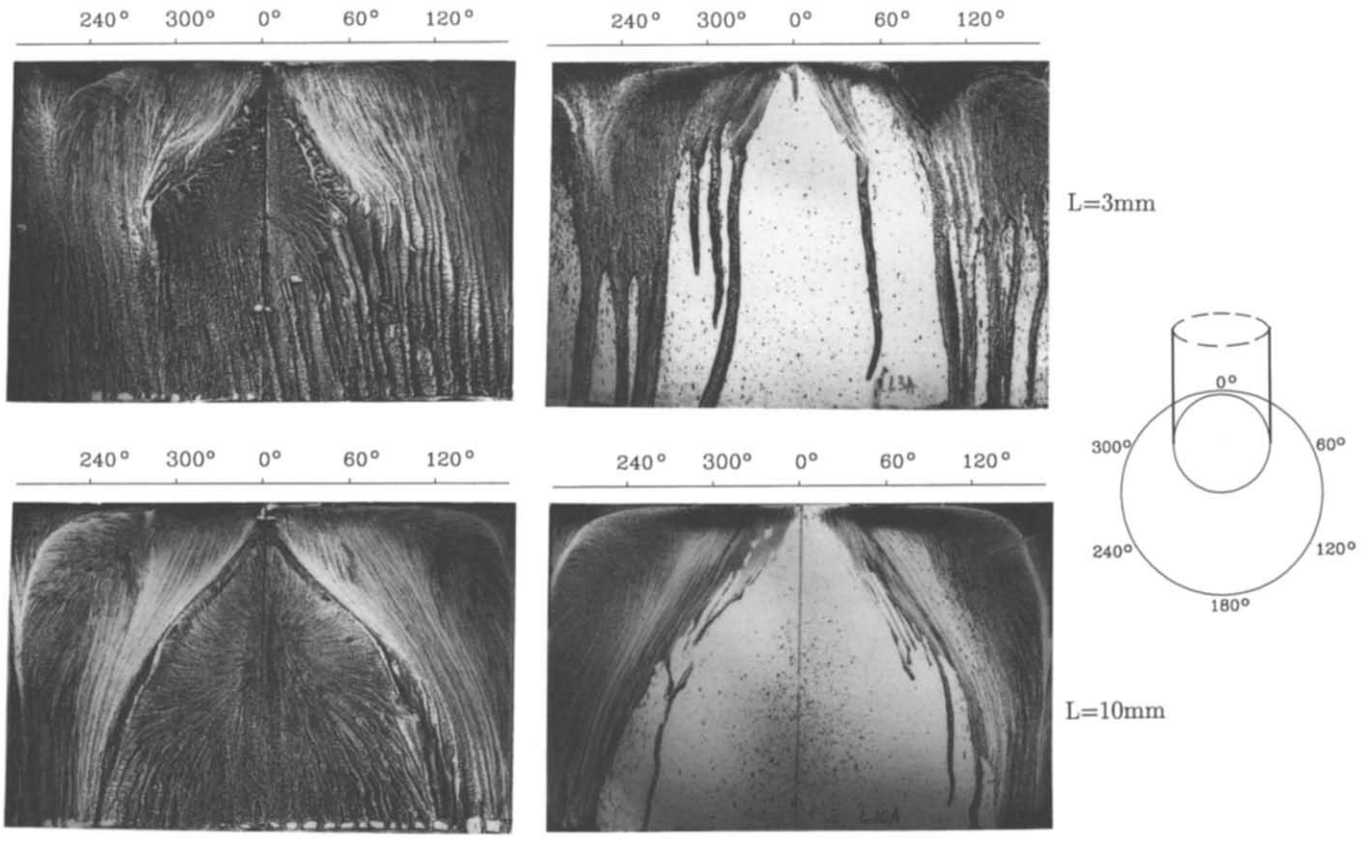

Figure 8 Time-averaged flow pattern on the cylinder wall for two valve lifts and maximum valve offset (valve type I, $\Delta p = 1960$ Pa). Left: overall flow pattern; right: discharge process

maximum ($L = 10$ mm) and middle ($L = 5$ mm) valve lifts, the flow in the central part of the head is deflected toward the left-hand side of the symmetry plane (0°–180°). At low lift ($L = 3$ mm), the flow is more nearly symmetric. On the opposite side from the port, the streak lines suggest radial outflow from the valve over an azimuthal range that increases with decreasing valve lift.

Asymmetric flow for maximum valve offset is also indicated in time-averaged flow patterns on the cylinder wall (see Figure 8). This figure includes flow patterns found both by painting the wall (left) and injecting the oil through the valve (right). The patterns on the left suggest that the flow developing down the cylinder becomes more nearly symmetric relative to the symmetry plane at higher valve lifts; however, the corresponding patterns of the discharge indicate an asymmetric process in each case. With increasing valve lift, the discharge from the valve into the cylinder occupies a wider range of the cylinder periphery. For the test conditions used in this experiment ($\Delta p = 1960$ Pa and $L = 3$ mm), the Reynolds number (based on the valve inner seat diameter) is on the order of 12×10^3, and the flow is not fully turbulent. The transitional flow within the inlet port can be expected to affect the flow in the cylinder.

In the case of half-valve offset, the time-averaged flow patterns on the cylinder head at three valve lifts are shown in Figure 9. The flow is less organized than that for maximum valve offset, and there is a much stronger dependence of the flow patterns on the valve lifts, probably due to the bigger space between the valve and the cylinder wall (minimum distance 11.5 mm compared with about 1 mm with the maximum valve offset). At low lift (Figure 9c), the flow separates around most of the valve circumference. At higher valve lift, the azimuthal extent of the separated flow around the valve periphery is strongly reduced, and the flow is highly asymmetric. At

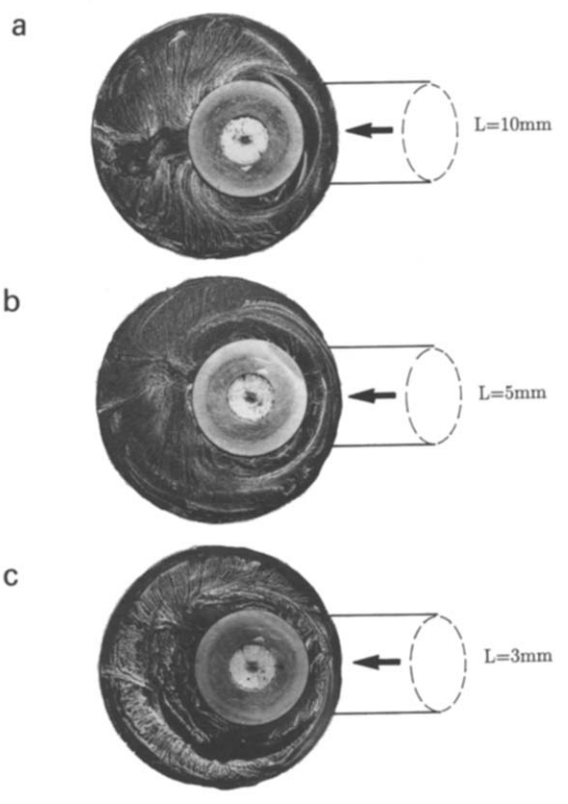

Figure 9 Time-averaged flow pattern on the cylinder head face for three valve lifts and half of maximum valve offset (valve type I, $\Delta p = 1960$ Pa)

$L = 5$ mm (Figure 9b), only a very small region of radial outflow from the valve is indicated, and its location is significantly deflected from the symmetry plane. At maximum valve lift (Figure 9a), the flow-separation region around the valve is further reduced, and radial outflow from the valve along the 0°-line is indicated.

The time-averaged flow patterns on the cylinder wall (Figure 10) also show that the flow is not symmetrically distributed around the symmetry plane, and that the valve lift has a noticeable influence on the flow distribution. The tangential flow characterized by two opposing jets (clearly observed for maximum valve offset) is strongly reduced, especially at higher distances from the head and low valve lift.

For the head with an on-axis valve, the flow patterns on the head (Figure 11) and cylinder walls (Figure 12) confirmed near zero-swirl flow, especially at higher valve lifts. The jets impinging on the cylinder wall (almost parallel to the head regardless of the valve lift) suggest a uniform discharge rate with a constant discharge angle around the valve periphery.

4. Concluding remarks

(1) The in-cylinder flow for a geometrically symmetric head configuration and off-axis valve location is asymmetric. The asymmetry increases with increasing valve lift and valve offset.

(2) Axial velocity measurements near the cylinder wall quantify the asymmetry around the cylinder periphery. Axial

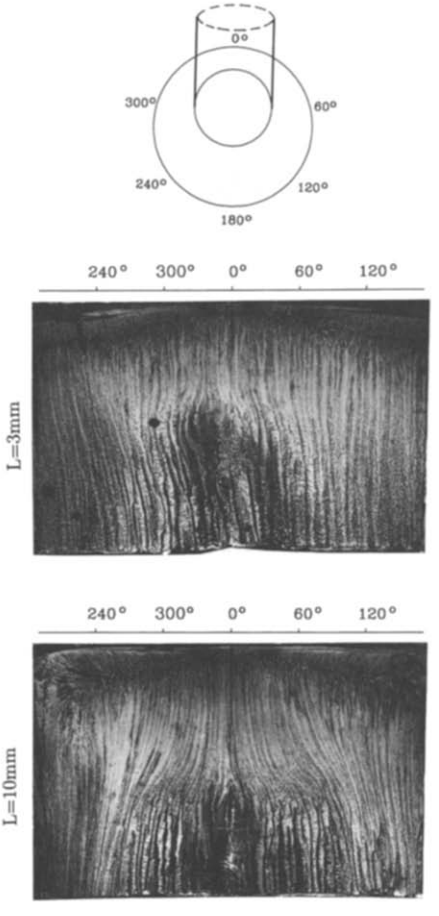

Figure 10 Time-averaged flow pattern on the cylinder wall for half of maximum valve offset at two valve lifts (valve type I, $\Delta p = 1960$ Pa)

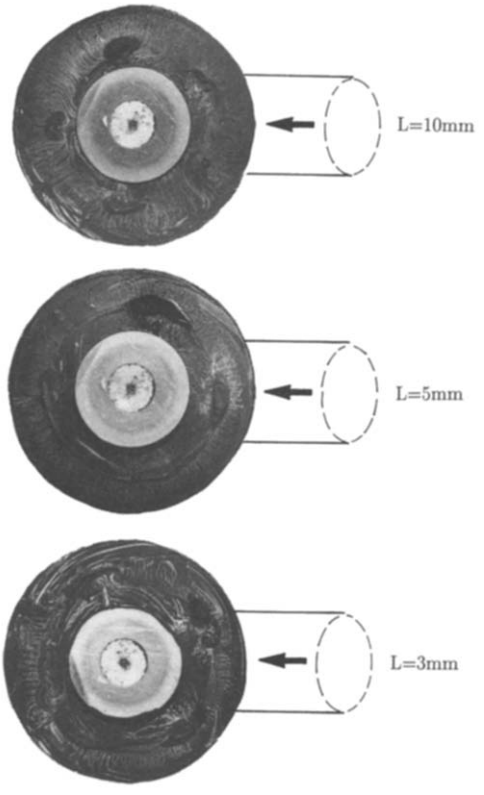

Figure 11 Time-averaged flow pattern on the cylinder head face for three valve lifts and on-axis valve (valve type I, $\Delta p = 1960$ Pa)

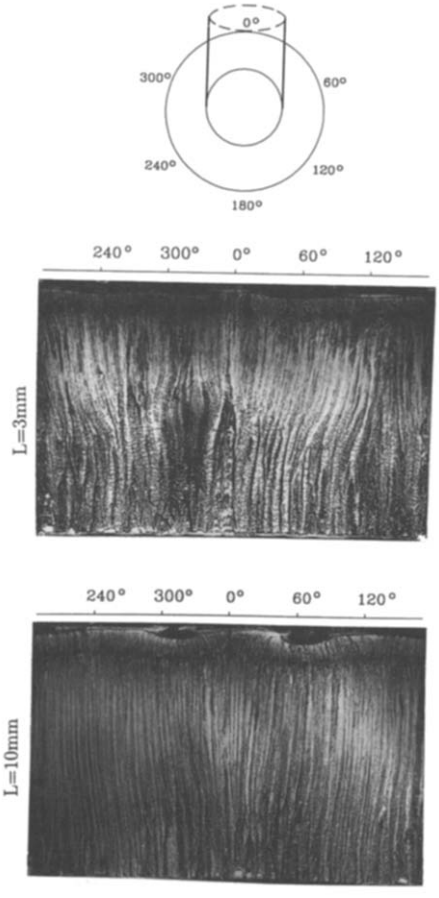

Figure 12 Time-averaged flow pattern on the cylinder wall for on-axis valve at two valve lifts (valve type I, $\Delta p = 1960$ Pa)

velocity and turbulence intensity distributions around the cylinder are only slightly dependent on the distance from the head.

(3) The flow asymmetry is thought to be due to flow separation in the bent inlet pipe and at the valve, causing asymmetric discharge into the cylinder. It was not feasible to make velocity measurements in the inlet port to check this supposition.

(4) The flow asymmetry in the cylinder is not due to misalignment of the inlet port around the symmetry plane or to eccentricity of the valve in the inlet port. The asymmetry is a characteristic feature of flow in the cylinder for off-axis valve locations.

(5) The characteristic flow asymmetry for geometrically symmetric head configurations with off-axis valve location is an important consideration for CFD simulations of the in-cylinder flow. Realistic flow predictions will require boundary conditions, e.g., in the valve gap, that adequately describe the local asymmetry of the flow.

(6) Combined application of surface-flow visualization techniques and laser-Doppler anemometry allows both qualitative and quantitative maps of the flow field inside the cylinder. The relatively rapid flow visualization experiments complement precise but time-consuming LDA measurements.

Acknowledgment

Financial support for this work was provided by a grant from Ford Werke AG, Cologne, Germany. The authors are also grateful to Dr. A. H. Brohmer of Ford AG for very useful discussions. Part of the work was also supported by a grant from the German Research Council (DFG)-Project We 1758/1-1.

References

Ahmadi-Befrui, B., Gosman, A. D., and Watkins, A. P. 1984. Prediction of in-cylinder flow and turbulence with three versions of k–ε turbulence model and comparison with data. *Flows in Internal Combustion Engines* (Vol. II). ASME, New York, 27–37

Annand, W. J. D. and Roe, G. E. 1974. *Gas Flow in the Internal Combustion Engine*. Foulis, Yeovil, UK

Arcoumanis, C., Bicen, A. F., Vafidis, C., and Whitelaw, J. H. 1984. Three-dimensional flowfield in motored reciprocating engines. *SAE Trans.*, **96**, 5.978, SAE Technical Paper, no. 841360

Arcoumanis, C. and Whitelaw, J. H. 1987. Fluid mechanics of internal combustion engines—a review. *Proc. I. Mech. Eng.*, **201**, (C1)

Brandstätter, W., Johns, R. J. R., and Wigley, G. 1985. The effect of inlet port geometry on in-cylinder flow structure. SAE Technical Paper, no. 850499

Ekchian, A. and Hoult, D. P. 1979. Flow visualization study of the intake process of an internal combustion engine. SAE Technical Paper, no. 790095, Detroit

Gosman, A. D. 1985. Multidimensional modeling of cold flows and turbulence in reciprocating engines. SAE Technical Paper, no. 850344, Detroit

Gosman, A. D., Johanbakhsh, A., and Watkins, A. P. 1985. Evaluation of multidimensional predictions of flow in piston-bowl configurations. *Proc. ASME Winter Meeting*, Miami, 115

Gosman, A. D., Melling, A., Whitelaw, J. H., and Watkins, A. P. 1978. Axisymmetric flow in a motored reciprocating engine. *Proc. I. Mech. Eng.*, **192** (11), 213

Hirotomi, T., Nagayama, I., Kobayashi, S., and Yamamasu, M. 1981. Study of induction swirl in a spark ignition engine. SAE Technical Paper, no. 810496, Detroit

Kent, J. C., Mikulec, A., Rimai, L., Adamczyk, A. A., Mueller, S. R., Stein, R. A., and Warren, C. C. 1989. Observations on the effects of intake-generated swirl and tumble on combustion duration. SAE Technical Paper, no. 892096, Detroit

Khalighi, B. 1990. Intake-generated swirl and tumble motions in a 4-valve engine with various intake configurations—flow visualization and particle tracking velocimetry. SAE Technical Paper, no. 900059, Detroit

Khalighi, B., El Tahry, S. H., and Kuziak, W. R. Jr. 1986. Measured steady flow velocity distributions around a valve/seat annulus. SAE Technical Paper, no. 860462, Detroit

Lee, K. C., Suen, K. O., Yianneskis, M., and Ganti, G. 1992. Steady flow characteristics of two generic inlet ports. *Sixth Int. Symp. Appl. Laser Techniques to Fluid Mechanics, Lisbon* (paper 29)

Monaghan, M. L. and Pettifer, H. F. 1981. Air motion and its effect on Diesel engine performance and emissions. SAE Technical Paper, no. 810255, Detroit

Paul, E. M. 1987. Numerical prediction of fluid motion in the induction system and the cylinder in reciprocating engines. SAE Technical Paper, no. 870594, Detroit

Stieglmeier, M. and Tropea, C. 1992. Mobile fiber-optic laser Doppler anemometer. *Appl. Optics*, **31**, 4096–4105

Takenaka, Y., Yabe, M., Aoyagi, Y., and Shiozaki, T. 1990. Three dimensional computation of in-cylinder flow with intake port in DI Diesel engine. *Proc. Int. Symp. COMODIA '90*, 425–430, Kyoto

Tanaka, K. 1929. Air flow through suction valve of conical seat. Report, parts 1 and 2, Aeronautical Research Institute, Tokyo

Tsui, Y. Y. and Lee, S. Y. 1992. Calculation of turbulent flow through engine inlet ports. *Int. J. Heat Fluid Flow*, **13** (3), 232–240

Węcłaś, M., Melling, A., and Durst, F. 1993. Combined application of surface flow visualization and laser Doppler anemometry to engine intake flows. *Exp. Fluids*, **15**, 323–331